

# Probing the hotspot interaction length in NbN nanowire superconducting single photon detectors

J. J. Renema, R. Gaudio, Q. Wang, A. Gaggero, F. Mattioli, R. Leoni, M. P. van Exter, A. Fiore, and M. J. A. de Dood

Citation: [Appl. Phys. Lett.](#) **110**, 233103 (2017); doi: 10.1063/1.4984816

View online: <https://doi.org/10.1063/1.4984816>

View Table of Contents: <http://aip.scitation.org/toc/apl/110/23>

Published by the [American Institute of Physics](#)

---

## Articles you may be interested in

[Optically probing the detection mechanism in a molybdenum silicide superconducting nanowire single-photon detector](#)

Applied Physics Letters **110**, 083106 (2017); 10.1063/1.4977034

[Picosecond superconducting single-photon optical detector](#)

Applied Physics Letters **79**, 705 (2001); 10.1063/1.1388868

[Graphene-based optically transparent dipole antenna](#)

Applied Physics Letters **110**, 233102 (2017); 10.1063/1.4984956

[Frequency-multiplexed bias and readout of a 16-pixel superconducting nanowire single-photon detector array](#)

Applied Physics Letters **111**, 032603 (2017); 10.1063/1.4993779

[Bias sputtered NbN and superconducting nanowire devices](#)

Applied Physics Letters **111**, 122601 (2017); 10.1063/1.4990066

[Electron and thermal transport via variable range hopping in MoSe<sub>2</sub> single crystals](#)

Applied Physics Letters **110**, 233108 (2017); 10.1063/1.4984953

---

PHYSICS TODAY

WHITEPAPERS

## MANAGER'S GUIDE

Accelerate R&D with  
Multiphysics Simulation

READ NOW

PRESENTED BY

 COMSOL

# Probing the hotspot interaction length in NbN nanowire superconducting single photon detectors

J. J. Renema,<sup>1,a)</sup> R. Gaudio,<sup>2,a)</sup> Q. Wang,<sup>1</sup> A. Gaggero,<sup>3</sup> F. Mattioli,<sup>3</sup> R. Leoni,<sup>3</sup> M. P. van Exter,<sup>1</sup> A. Fiore,<sup>2</sup> and M. J. A. de Dood<sup>1</sup>

<sup>1</sup>Leiden Institute of Physics, Leiden University, Niels Bohrweg 2, 2333 CA Leiden, The Netherlands

<sup>2</sup>COBRA Research Institute, Eindhoven University of Technology, P.O. Box 513, 5600 MB Eindhoven, The Netherlands

<sup>3</sup>Istituto di Fotonica e Nanotecnologie (IFN), CNR, via Cineto Romano 42, 00156 Roma, Italy

(Received 11 July 2016; accepted 10 May 2017; published online 6 June 2017)

We measure the maximal distance at which two absorbed photons can jointly trigger a detection event in NbN nanowire superconducting single photon detector microbridges by comparing the one-photon and two-photon efficiencies of bridges of different overall lengths, from 0 to 400 nm. We find a length of  $23 \pm 2$  nm. This value is in good agreement with the size of the quasiparticle cloud at the time of the detection event. *Published by AIP Publishing.*

[<http://dx.doi.org/10.1063/1.4984816>]

Nanowire superconducting single photon detectors (SSPDs)<sup>1</sup> are a crucial technology for a variety of applications.<sup>2</sup> These devices consist of a thin superconducting film which detects photons when biased to a significant fraction of its critical current. Although details of the microscopic mechanism are still in dispute,<sup>3</sup> the present understanding of this process in Niobium Nitride (NbN) SSPDs is as follows:<sup>4–13</sup> after the absorption of a photon, a cloud of quasiparticles is created, which is known as a hotspot. This cloud diffuses, spreading out over some area of the wire. This causes the redistribution of bias current, which unbinds a vortex from the edge of the wire, if the applied bias current is such that the current for vortex entry is exceeded. The transition of a vortex across the wire creates a normal-state region, which grows under the influence of Joule heating from the bias current, leading to a voltage pulse and a detection event.<sup>14</sup>

Recently, applications of these detectors have been demonstrated or proposed, which rely on the ability of such devices to operate as multiphoton detectors, such as multiphoton subwavelength imaging,<sup>15</sup> ultrasensitive higher order autocorrelation,<sup>16</sup> and near-field multiphoton sensing.<sup>17</sup> These applications use the fact that when biased at lower currents than required for single-photon detection, the detector responds only when several photons are absorbed simultaneously.<sup>18</sup> Moreover, this multiphoton response was of great significance in investigating the question of the working mechanism of such devices.<sup>4</sup>

For the multiphoton process to be efficient, the two photons must be absorbed within some given distance of each other along the length of the wire, which we will refer to as the *hotspot interaction length*  $s$ . Akhlaghi and Majedi showed<sup>19</sup> that this can be modeled as a combinatoric process, where one conceptually divides a long nanowire into many bins and posits that a detection only occurs when two photons land in the same bin. With this model, one can compute the detection probability in the multiphoton regime from the

one-photon detection efficiency and the combinatorics of this process, demonstrating that this is the mechanism which determines the efficiency in this detection regime. Photons which are absorbed far away from each other along the wire will not be able to jointly cause a detection event.

In this work, we use this effect to measure the hotspot interaction length. Our experiment is based on comparing the detector response in the one-photon and two-photon regimes of a series of uniformly illuminated nanowires of different lengths [see Fig. 1(a)]. We rely on quantum detector tomography<sup>20</sup> (QDT) to find the bias currents at which the one and two-photon regimes occur. We experimentally find a hotspot interaction length of  $s = 23 \pm 2$  nm. We find that the tapers leading to our nanowires are photodetecting over a length of approximately  $35 \pm 6$  nm on each side.

We interpret these results in terms of the diffusion-based vortex crossing model of the detection event. We show that the measured hotspot interaction length corresponds to the computed size of the quasiparticle cloud at the

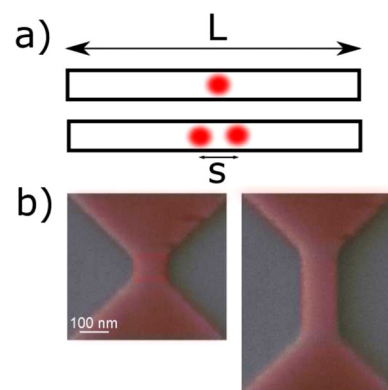


FIG. 1. (a) Sketch of the experiment. Top panel: a nanowire of length  $L$  is illuminated uniformly, and the current the nanowire is set to be in the single-photon regime. Photon absorption at any point in the wire is sufficient to cause a detection event. In the bottom panel, the detector is in the two-photon regime, and a detection is observed only if the second photon is absorbed in the region (red spot) where an excess quasiparticle concentration has been created by the first photon. (b) False color SEM images of two nanowires of  $L = 100$  nm and  $L = 400$  nm, respectively.

<sup>a)</sup>J. J. Renema and R. Gaudio contributed equally to this work.

moment of a detection event, which demonstrates the agreement between our experiment and our numerical model. Finally, we discuss the implications of these results for multiphoton-based SSPD applications.

To characterize these detectors optically, we perform QDT.<sup>20,23–25</sup> In QDT, the detector is illuminated with a set of known probe states. By measuring the count rate as a function of bias current and combining this with the photon number distribution as a function of mean photon number  $N$ , we can measure the probability of a detection event given  $n$  incident photons. In this general description, the count rate is given by

$$R_{\text{click}} = e^{-\eta N} \sum_{n=0}^{\infty} \frac{(\eta N)^n}{n!} p_n, \quad (1)$$

where  $\eta$  is a linear efficiency parameter and  $\{p_n\}$  are series of nonlinear parameters which correspond to the detection probability of  $n$  photons. For SSPDs, which are threshold detectors, there is some  $n_{th}$  for which  $p_n \approx 1$  for all  $n \geq n_{th}$ , which defines the photon regime of the wire. We will refer to  $\eta_n$  as shorthand for  $\eta$  in the  $n$ -photon regime and all efficiencies are defined as single-photon efficiencies. For nanobridges, we showed that  $\eta$  is roughly constant with bias current and that the resulting value for those devices is consistent with the optical absorption into the detector. However, we noted<sup>23</sup> that our parameterization does not

distinguish between linear loss inside the detector and outside of it. In this letter, we show that the effect of a finite hotspot interaction length manifests itself as a photon-regime dependent linear efficiency in SSPDs with nonzero wire length.

To characterize a device, we apply our tomography protocol to count rate measurements at each bias current individually. In practice, Eq. (1), which contains infinitely many parameters, needs to be made suitable for fitting by use of model selection.<sup>23</sup>

Figure 2(a) shows the result of this characterization on a 100  $\mu\text{m}$  long NbN detector on  $\text{SiO}_2$  (see Ref. 25 for details). The striking difference between this result and our previous characterization of nanobridges [see also Figs. 2(b) and 2(c)]<sup>23</sup> is that for the meander, the linear efficiency parameter  $\eta$  is a strong function of bias current, while in the case of the nanobridges it is nearly constant.

Since we know that the count rate in the multiphoton regime is determined by the statistics of the hotspot overlap, we conclude that for a wire of nonzero length, the finite size of the hotspot manifests itself in the reduction of  $\eta$  with bias current. This analysis is consistent with the approach of Ref. 19, where the photon number regime (quantified by  $p_n$  in our parametrization) was used to identify the number of hotspots which must overlap, and the efficiency was used to compute the probability that this occurs. Such a straightforward interpretation of the efficiency is only possible in the

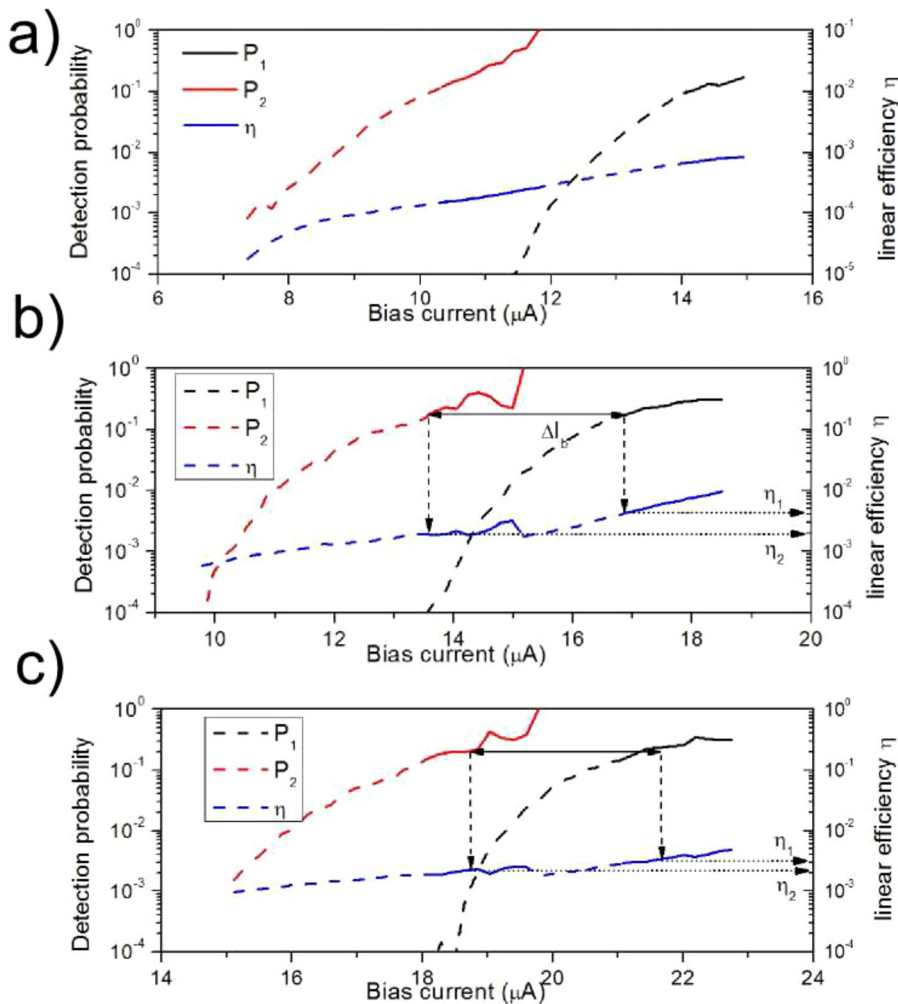


FIG. 2. Full tomographic characterization of a meander detector (*top*), the  $L=400$  nm sample (*middle*), and the  $L=0$  nm sample (*bottom*). The black and red lines show the nonlinear detection probabilities for single photons ( $p_1$ ) and photon pairs ( $p_2$ ), respectively. The blue line shows the linear efficiency  $\eta$ . The solid parts of the curves are used in our analysis. The dashed arrows show how we obtain the ratio of efficiencies in the one- and two-photon regimes  $\eta_1/\eta_2$  for one particular value of  $p_n$ .

pure  $N$ -photon regime, where the count rate is dominated by a given multiphoton process.<sup>19</sup> We will restrict ourselves to these cases in the rest of this work.

It is, however, difficult to analyze this measurement in any quantitative way. For this experiment, it is crucial that the entire area of the detector is active. However, the device detection efficiency of our meander is a few percent, which indicates that our device is strongly inhomogeneous.<sup>21,22</sup> To remove these problems, we repeat our experiment on a series of short wires.

The detectors used in the rest of our experiments were patterned from a single film (5 nm NbN on GaAs) to ensure that the properties of the wires are as similar as possible. We fabricated 16 detectors of each length, with lengths of  $L = 0, 100, 200$ , and  $400$  nm. To avoid comparing dissimilar detectors, we measured the critical current of our devices and selected one for each length with critical currents between  $27.4$  and  $27.9 \mu\text{A}$ . This value is consistent with earlier samples,<sup>4,15,22,23</sup> including bridge samples (nanodetectors) which have a very low probability of containing a defect.

We used a Ti:Sapphire laser with a wavelength of  $\lambda = 800$  nm to perform our experiments. This laser has a pulse duration of approximately  $100$  fs, which is much shorter than the lifetime of an excitation in an SSPD.<sup>16</sup> This removes the temporal response of the nanowire from the problem. The laser is attenuated by a  $\lambda/2$  plate between two polarizers. The second polarizer is aligned to the long axis of the nanowire, resulting in almost uniform illumination across the wire.<sup>12</sup> The spot size was chosen to be much larger than the length of the wire, to ensure uniform illumination along the wire length.

Figures 2(b) and 2(c) show two typical experimental results for the  $L = 0$  and  $L = 400$  nm wires, respectively. Since these devices have a smaller active area, and hence lower efficiency, there is a higher statistical spread on the observed values of  $p_n$ . The results of these two devices are almost identical, apart from the linear efficiency  $\eta$ , which falls off faster for the longer wire, consistent with what we expected from Fig. 2(a).

As noted before,  $\eta$  only has a physically meaningful interpretation in the pure  $N$ -photon regimes. To find these points, we use the values of  $p_n$ , which indicate which photon number regime we are in. We compare like for like: we start by finding the value of  $\Delta I_b$  such that  $p_2(I_b) = p_1(I_b + \Delta I_b)$ , as shown in Fig. 2. We then take the ratio of efficiencies  $\eta_1/\eta_2 = \eta(I_b + \Delta I_b)/\eta(I_b)$ . This is illustrated in Fig. 2 for one particular value of  $p_n$ . As expected, we only find meaningful information in the pure photon regime: for currents where  $p_{1,2} \gtrsim 0.2$ , we find that the resulting ratio is independent of bias current and we restrict all further analysis to this regime (supplementary material).

Figure 3 shows the resulting values of  $\eta_1/\eta_2$  for  $L = 0$ – $400$  nm, from which we extract  $s$ . As expected, the two-photon regime becomes less efficient relative to the one-photon regime as the wire length is increased. The errors, which were estimated by considering the statistical spread observed in  $\eta_1$  and  $\eta_2$  in the regime  $p_n > 0.2$ , are more or less independent of the wire length. The low value of  $\eta_2$  strongly amplifies the error on the  $\eta_1/\eta_2$  ratio at  $400$  nm.

To find the hotspot length, we note that in the pure one-photon regime, we expect  $\eta_1 = CwL$ , where  $C$  is a constant

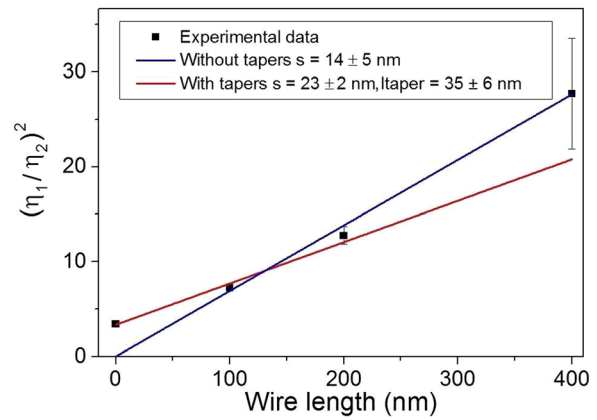


FIG. 3. Ratio of linear efficiencies  $\eta_1/\eta_2$  for the one and two-photon regimes, derived from tomography as shown in the previous figure. The blue line shows a fit which does not take into account photodetection events in the tapers leading to the wire. The straight lines are fits to the data that either neglect (blue line) or include (red line) an additional taper. From that fit, we find  $s = 23$  nm,  $L_{\text{taper}} = 35$  nm.

which contains the absorption per unit area into the wire and the overlap between our probe beam and the detector, and  $w$  and  $L$  are the width and length of the wire, respectively. For the two-photon regime, we similarly expect  $\eta_2^2 = C^2wLA$ , where  $A$  is the area within which the second photon must be absorbed. Motivated by the notion that when two photons are absorbed in the same cross-section of the wire, current continuity causes a direct, instantaneous interaction between the two photons that is independent of the absorption details.<sup>7</sup> We expect the effect of a photon absorption to extend along the entire width of the wire, so that we can write  $A = ws$ , where  $s$  is the hotspot interaction length. This is supported by previous experiments,<sup>4</sup> where we have observed that the two-photon regime for photons with energy  $E$  coincides with the one-photon regime for photons with energy  $2E$ . Using these expressions, we can construct the following expression for  $s$ :

$$L/s = (\eta_1/\eta_2)^2. \quad (2)$$

However, the equations which we have are unphysical for  $L = 0$ , where  $\eta_2 = \eta_1 = 0$ , as it neglects the possibility that photons absorbed close to the end of the wire can trigger a detection. We model this effect by substituting  $L_{\text{eff}} = L + 2L_{\text{taper}}$  into Eq. (2). Using this modified wire length, we find values of  $s_{\text{hs}} = 23 \pm 2$  nm and  $L_{\text{taper}} = 35 \pm 6$  nm. The red line shows the fit to Eq. (2), taking into account the finite size of the taper, whereas the blue line shows the fit without considering that of the taper. The observed value of  $L_{\text{taper}}$  is in reasonable agreement with earlier estimates of the active area of such nanobridges, which found  $L_{\text{taper}} \approx 50$  nm.<sup>15,23</sup>

In order to find out how our observed length scale fits in the physical picture of the detection event, we perform a series of numerical simulations in COMSOL of current continuity and quasiparticle diffusion, similar to those reported on Refs. 7 and 12. We have made three simplifications compared to these references. First, we have approximated the process of hot electron to Quasiparticle (QP) conversion as an exponentially decaying source of QP located at the photon



absorption site. Second, we have ignored the nonlinear interaction between the condensate velocity and the number of quasiparticles, which amounts to taking the limit of low quasiparticle densities and equivalently low photon energies. This later approximation is somewhat justified by the fact that we are in the regime where the energy-current relation is linear.<sup>4</sup> Third, in these simulations we only consider photon absorption events in the center of the wire. This is justified because when two photons are absorbed in the same cross-section of the wire, the interaction between the two of them is mediated instantaneously by current continuity, which dictates that the current diverted by one hotspot cannot flow through the other, and vice versa.

Figure 4 shows that the length scale which we have measured in our experiment is that of quasiparticle diffusion at the time of the detection event. We plot the maximum value of the current along the edge of the wire (in units of the applied bias current), which is the quantity that is known to determine whether a detection event occurs,<sup>7</sup> as a function of hotspot separation  $d$ . By finding where and when the current density along the wire is maximal, we can identify the position and time of the photodetection event. In the four insets, we plot the distribution of quasiparticles at the timestep when the maximum edge current is achieved and we indicate the position where this happens with a double red arrow.

The edge current is roughly constant up to  $d_{hs} \approx 15$ –20 nm and then starts to roll off. This roll-off occurs close to the observed value of  $s$ , which corresponds to the point when the quasiparticle clouds no longer significantly overlap. We therefore identify the observed hotspot interaction length with the size of the QP cloud.

We have shown that our value of  $s$  is consistent with that predicted by a model based on diffusion. Since the diffusion equation is linear, our model suggests that adding energy does not make the hotspot wider. This is in contrast to the result of Verevkin *et al.*,<sup>18</sup> who inferred an increase in the hotspot size based on the measurement of the threshold current. Instead, adding energy takes out a higher fraction of superconducting

electrons. This continues at most until at the center of the hotspot where the electrons are exhausted and a normal hotspot forms, which is predicted to occur for NbN at a photon energy of 2.5 eV.<sup>7</sup> If the hotspot is modeled as a static object with a finite temperature, there is a strong energy dependence,<sup>26</sup> since when we put more energy into the system, it takes longer for it to return below its critical temperature. These two models essentially consist of the limits of photon energy much smaller and much larger than the energy required to break the condensate.

From Fig. 4, we find that there has to be significant overlap between the two hotspots in order to jointly cause a detection event; the two hotspots must be closer together than their  $1/e$  width. If we approximate the size of the hotspot by its diffusion length, this result enables us to convert  $s$  into a time-scale, since the diffusion constant for quasiparticles is known<sup>7</sup> to be  $D = 0.4$ – $0.6$  cm<sup>2</sup>/s. Using the relation  $s = \sqrt{Dt}$ , we find a value of  $t_{det} = 2.7 \pm 0.6$  ps. This is in good agreement with the value predicted in Ref. 7 for the time at which a detection event happens. In a range of  $d = 20$ – $60$  nm, the two absorbed photons still interact through the current continuity condition. Essentially, the current crowding caused by the first QP cloud has not healed before the current encounters the second QP cloud. However, this length scale is not visible in Fig. 4: the edge current decreases smoothly for  $d > 20$  nm. We therefore conclude that it is the length scale set by the QP cloud that determines  $s$ .

We speculate that the reason we find a slightly shorter length scale in our simulations than our experiment is because we only consider photons absorbed on the central axis of the wire. It is known that photons which are absorbed at the edges are more efficient at causing detection events.<sup>10,12</sup> A full simulation of all possible two-photon absorption configurations is beyond the scope of this work; our purpose here is to show the plausibility of our interpretation of the observed length scale.

Our result implies that increasing the length of the wire will increase the probability of multiphoton events, but each  $\sim 20$  nm long segment of the wire will act as an independent multiphoton detector. For a typical 100  $\mu$ m long SSPD, the overall detection probability in the two-photon regime would be  $10^{-4}$  lower than in the single-photon regime. The only way to obtain highly efficient multiphoton detection in SSPDs is to use far-subwavelength focussing, e.g., by using nano-antennas.

Recently, a similar experiment was performed on WSi, which found that the experimental data on two-photon pump-probe measurements<sup>26</sup> could be well explained by a static hotspot of  $s > 100$  nm. It is possible that self-confinement of the hotspot plays a larger role in Tungsten Silicide (WSi) than in NbN due to the larger fraction of Cooper pairs which are destroyed in the former material. This would be evidence of a qualitative difference in the detection mechanism between NbN and WSi SSPDs.

In conclusion, we have observed that the size of an excitation in NbN SSPDs is approximately 23 nm. We have shown that this number can be interpreted as the size of the quasiparticle cloud at the moment of detection. This observation is consistent with the predictions of the diffusion-based vortex crossing model.

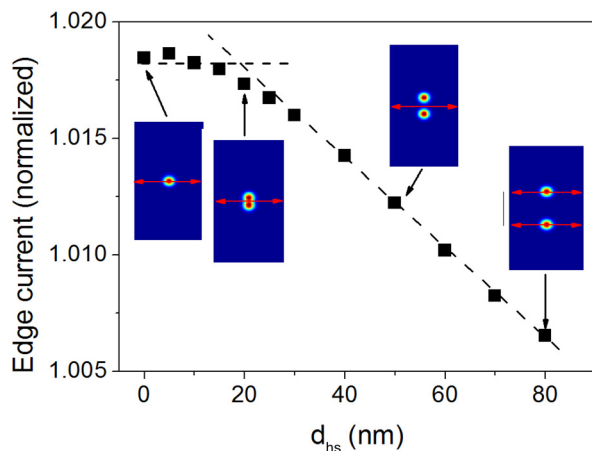


FIG. 4. Simulated edge current as a function of photon absorption separation, normalized to the applied bias current. The dashed lines are guides to the eye. The insets show the quasiparticle distribution at the moment of maximum edge current, which we associate with the detection event. The arrows indicate the point where the edge current is maximal.

See [supplementary material](#) for details of the fabrication, tomography, and the dependence of our result on film thickness.

We thank E. Driessen, A. Kozorezov, D. Vodolazov, M. Stevens, F. Marsili, and A. Engel for useful discussions. This work is part of the research programme of the Foundation for Fundamental Research on Matter (FOM), which was financially supported by the Netherlands Organisation for Scientific Research (NWO) and was also supported by NanoNextNL, a micro- and nanotechnology program of the Dutch Ministry of Economic Affairs, Agriculture and Innovation (EL&I) and 130 partners. J.J.R. acknowledges support of D. Bouwmeester's NWO Spinoza award.

- <sup>1</sup>G. N. Goltsman, O. Okunev, G. Chulkova, A. Lipatov, A. Semenov, K. Smirnov, B. Voronov, A. Dzardanov, C. Williams, and R. Sobolewski, "Picosecond superconducting single-photon optical detector," *Appl. Phys. Lett.* **79**(6), 705 (2001).
- <sup>2</sup>C. M. Natarajan, M. G. Tanner, and R. Hadfield, "Superconducting nanowire single-photon detectors: Physics and applications," *Supercond. Sci. Technol.* **25**(6), 063001 (2012).
- <sup>3</sup>A. Engel, J. Renema, K. Il'in, and A. Semenov, "Detection mechanism of superconducting nanowire single-photon detectors," *Supercond. Sci. Technol.* **28**(11), 114003 (2015).
- <sup>4</sup>J. J. Renema, R. Gaudio, Q. Wang, Z. Zhou, A. Gaggero, F. Mattioli, R. Leoni, D. Sahin, M. J. A. de Dood, A. Fiore, and M. P. van Exter, "Experimental test of theories of the detection mechanism in a nanowire superconducting single photon detector," *Phys. Rev. Lett.* **112**, 117604 (2014).
- <sup>5</sup>D. Y. Vodolazov, "Saddle point states in two-dimensional superconducting films biased near the depairing current," *Phys. Rev. B* **85**, 174507 (2012).
- <sup>6</sup>A. N. Zotova and D. Y. Vodolazov, "Photon detection by current-carrying superconducting film: A time-dependent Ginzburg-Landau approach," *Phys. Rev. B* **85**, 024509 (2012).
- <sup>7</sup>A. Engel and A. Schilling, "Numerical analysis of detection-mechanism models of superconducting nanowire single-photon detector," *J. Appl. Phys.* **114**(21), 214501 (2013).
- <sup>8</sup>J. J. Renema, G. Frucci, Z. Zhou, F. Mattioli, A. Gaggero, R. Leoni, M. J. A. de Dood, A. Fiore, and M. P. van Exter, "Universal response curve for nanowire superconducting single-photon detectors," *Phys. Rev. B* **87**, 174526 (2013).
- <sup>9</sup>R. Lusche, A. Semenov, K. Ilin, M. Siegel, Y. Korneeva, A. Trifonov, A. Korneev, G. Goltsman, D. Vodolazov, and H.-W. Hübers, "Effect of the wire width on the intrinsic detection efficiency of superconducting-nanowire single-photon detectors," *J. Appl. Phys.* **116**(4), 043906 (2014).
- <sup>10</sup>A. N. Zotova and D. Y. Vodolazov, "Intrinsic detection efficiency of superconducting single photon detector in the modified hot spot model," *Supercond. Sci. Technol.* **27**, 125001 (2014).
- <sup>11</sup>D. Y. Vodolazov, "Current dependence of the red boundary of superconducting single-photon detectors in the modified hot-spot model," *Phys. Rev. B* **90**, 054515 (2014).
- <sup>12</sup>J. J. Renema, Q. Wang, R. Gaudio, I. Komen, K. op 't Hoog, D. Sahin, A. Schilling, M. P. van Exter, A. Fiore, A. Engel, and M. J. A. de Dood, "Position-dependent local detection efficiency in a nanowire superconducting single-photon detector," *Nano Lett.* **15**, 4541 (2015).
- <sup>13</sup>A. G. Kozorezov, C. Lambert, F. Marsili, M. J. Stevens, V. B. Verma, J. A. Stern, R. Horansky, S. Dyer, S. Duff, D. P. Pappas, A. Lita, M. D. Shaw, R. P. Mirin, and S. W. Nam, "Quasiparticle recombination in hot-spots in superconducting current-carrying nanowires," *Phys. Rev. B* **92**, 064504 (2015).
- <sup>14</sup>A. J. Kerman, E. A. Dauler, W. E. Keicher, J. K. W. Yang, K. K. Berggren, G. Goltsman, and B. Voronov, "Kinetic-inductance-limited reset time of superconducting nanowire photon counters," *Appl. Phys. Lett.* **88**(11), 111116 (2006).
- <sup>15</sup>D. Bitauld, F. Marsili, A. Gaggero, F. Mattioli, R. Leoni, S. Jahanmirinejad, F. Lévy, and A. Fiore, "Nanoscale optical detector with single-photon and multiphoton sensitivity," *Nano Lett.* **10**(8), 2977–2981 (2010).
- <sup>16</sup>Z. Zhou, G. Frucci, F. Mattioli, A. Gaggero, S. Jahanmirinejad, T. B. Hoang, and A. Fiore, *Phys. Rev. Lett.* **110**, 133605 (2013).
- <sup>17</sup>Q. Wang and M. J. A. de Dood, "An absorption-based superconducting nano-detector as a near-field optical probe," *Opt. Express* **21**, 3682 (2013).
- <sup>18</sup>A. Verevkin, J. Zhang, R. Sobolewski, A. Lipatov, O. Okunev, G. Chulkova, A. Korneev, K. Smirnov, and G. N. Gol'tsman, "A. Semenov Detection efficiency of large-active-area NbN single-photon superconducting detectors in the ultraviolet to near-infrared range," *Appl. Phys. Lett.* **80**, 4687 (2002).
- <sup>19</sup>M. K. Akhlaghi and A. H. Majedi, "Semiempirical modeling of dark count rate and quantum efficiency of superconducting nanowire single-photon detectors," *IEEE Trans. Appl. Supercond.* **19**(3), 361–366 (2009).
- <sup>20</sup>J. S. Lundeen, A. Feito, H. Coldenstrodt-Ronge, K. L. Pregnell, C. Silberhorn, T. C. Ralph, J. Eisert, M. B. Plenio, and I. A. Walmsley, "Tomography of quantum detectors," *Nat. Phys.* **5**(1), 27–30 (2009).
- <sup>21</sup>A. J. Kerman, E. A. Dauler, J. K. W. Yang, K. M. Rosfjord, V. Anant, K. K. Berggren, G. N. Goltsman, and B. M. Voronov, "Constriction-limited detection efficiency of superconducting nanowire single-photon detectors," *Appl. Phys. Lett.* **90**(10), 101110 (2007).
- <sup>22</sup>R. Gaudio, K. P. M. op 't Hoog, Z. Zhou, D. Sahin, and A. Fiore, "Inhomogeneous critical current in nanowire superconducting single-photon detectors," *Appl. Phys. Lett.* **105**, 222602 (2014).
- <sup>23</sup>J. J. Renema, G. Frucci, Z. Zhou, F. Mattioli, A. Gaggero, R. Leoni, M. J. A. de Dood, A. Fiore, and M. P. van Exter, "Modified detector tomography technique applied to a superconducting multiphoton nanodetector," *Opt. Express* **20**(3), 2806–2813 (2012).
- <sup>24</sup>J. S. Lundeen, K. L. Pregnell, A. Feito, B. J. Smith, W. Mauerer, C. Silberhorn, J. Eisert, M. B. Plenio, and I. A. Walmsley, "A proposed testbed for detector tomography," *J. Mod. Opt.* **56**(2–3), 432 (2009).
- <sup>25</sup>Q. Wang, J. J. Renema, A. Gaggero, F. Mattioli, R. Leoni, M. P. van Exter, and M. J. A. de Dood, "How noise affects quantum detector tomography," *J. Appl. Phys.* **118**(13), 134501 (2015).
- <sup>26</sup>F. Marsili, M. Stevens, A. Kozorezov, V. B. Verma, C. Labert, J. A. Stern, R. Horansky, S. Dyer, S. Duff, D. P. Pappas, A. Lita, M. D. Shaw, R. P. Mirin, and S. W. Nam, "Hotspot relaxation dynamics in a current carrying superconductor," *Phys. Rev. B* **93**, 094518 (2016).